CORELAȚII COMPOZIȚIE – PROCESARE – MICROSTRUCTURĂ LA CLINCHERE. IMPLICAȚII
CORRELATIONS COMPOSITION-PROCESSING-MICROSTRUCTURE ON SOME CLINKERS. IMPLICATIONS

ZENO GHIZDĂVEȚ[1], DANIELA NĂSTAC[2], MIHAI EFTIMIE[1]*, B. ȘTEFAN[1], IONELA STANCIU[1], ADRIAN VOLCEANOV[1]

[1] *University POLITEHNICA Bucharest, Splaiul Independentei Street, No. 313, Bucharest, Romania*
[2] *CEPROCIM S.A., Preciziei Street, Sector 6, Bucharest, Romania*

Multivariate Analysis (MVA) on a complex database has been performed, aiming to reveal correlations composition-processing conditions-microstructure for some clinkers. Database was made of cement clinker chemical analysis, information extracted from image analysis on clinker micrographs and clinkering plant process parameters. Clinkers were burned in different conditions in industry (19) or in laboratory (14 different clinkers in two groups). Image analysis of each clinker has been made by computing Shape Parameters, Fractal Dimension and a parameter derived from Shannon Entropy, called the Uniformity Degree. Also, the intermixed C_3A and C_4AF minerals as interstitial phase of the clinkers have been isolated and analyzed. MVA results clearly identified the influential parameters on the database. It was found that the free CaO content in clinker was influential on both composition-microstructure and process parameters. Therefore, we concluded that the free CaO can be seen as a link between laboratory and industrial parameters in understanding these complex correlations.

Analiza multivariată a unei baze de date complexe a evidențiat corelații compoziție-condiții de procesare-microstructură pentru anumite clinchere. Baza de date a fost constituită din rezultatele de analiză chimică ale unor clinchere de ciment, informații extrase din analiza imaginilor de microscopie optică a clincherelor și o serie de parametri de proces pentru instalația de clincherizare. Clincherele au fost arse în condiții diferite în industrie (19) sau în laborator (14 clinchere). Analiza imaginilor pentru fiecare clincher a constat în calculul parametrilor de formă, dimensiunii fractale și a unui parametru derivat din entropia Shannon, denumit Grad de Uniformitate. Au fost izolate și analizate în imaginile de microscopie optică fazele C_3A și C_4AF care constituie faza interstițială. Rezultatele finale ale analizei au identificat în mod clar cei mai importanți parametri din baza de date disponibilă. S-a constatat, de asemenea, că există un element-pivot – conținutul de CaO liber – între verigile compoziție, procesare și microstructură. Concluzia imediată este că oxidul de calciu liber poate fi un element de legatură între analizele de laborator și parametrii industriali în înțelegerea unor astfel de corelații complexe.

Keywords: *Image Analysis, Multivariate Analysis, clinker, optical microscopy, Shannon entropy, Fractal Dimension, Interstitial Phase*

1. Introduction

Cement clinkers contain mainly alite (roughly tricalcium silicate, $3CaO \cdot SiO_2$, C_3S), belite (roughly dicalcium silicate, $2CaO \cdot SiO_2$, C_2S) and interstitial phase (tricalcium aluminate, $3CaO \cdot Al_2O_3$, C_3A and tetracalcium aluminoferrite, $4CaO \cdot Al_2O_3 \cdot Fe_2O_3$, C_4AF). The proportion in which these minerals appear in clinker and the size and shape of the crystals influence clinker grindability and the mechanical properties of the cement and they are influenced, at their turn, by the raw materials features and by the processing conditions. Therefore, microstructure plays a pivotal role when investigating the quality of the clinker and all the influences that act upon it. One way to investigate microstructure is by using optical microscopy. Optical microscopy requires realistic image analysis to characterize minerals in clinker, while providing valuable information that can be further used in correlations.

Shape factors (particle shape parameters) are widely used to describe particles morphology (morphology has been described in [1] as referring to both shape and surface texture) due to various advantages [2, 3], the most important being that one can select the best suited parameter to explain the features of a population of particles. Disadvantages also exist when employing shape parameters, such as one has to carefully select the position of the particle relative to the caliper, when measuring.

In this paper, we will compute and use some of these shape factors on clinker microscopy images; we will add to these factors also the *Fractal*

* Autor corespondent/*Corresponding author*,
E-mail: mihai.eftimie@upb.ro

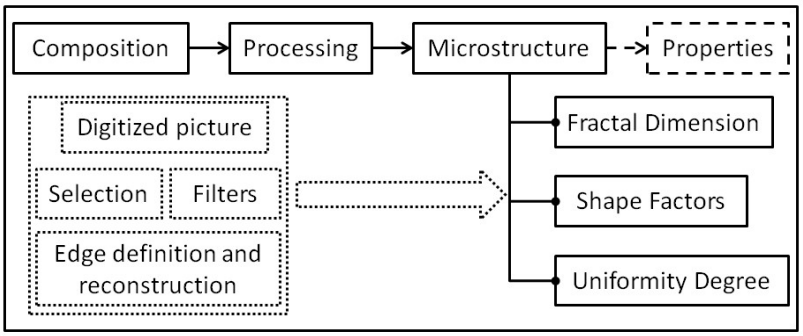

Fig. 1 - Sketch of the workflow within Composition-Processing-Microstructure-Properties chain. We did not address correlations with Properties in this article. / Corelația Compoziție-Procesare-Microstructura-Proprietăți. În această lucrare nu a fost realizată și corelația cu proprietățile de material.

Dimension (*FD*)[4, 5] and a parameter derived from *Shannon entropy*, called *Uniformity Degree* (U_H). While shape factors are - the most of them - related to shape, FD has been chosen as containing simultaneously shape information and size of the particles; UD provides information only about particles size distribution. These parameters will be examined and correlated for a number of industrial and laboratory made clinkers; some other parameters will be included in our analysis, such as chemical and phase composition analysis and also some technological parameters coming from the processing stage in the clinkering plant. Various techniques will be used to distill information from datasets, starting from image analysis techniques and *Fractal Dimension* calculation to up to *Self-Organizing Maps* (SOMs) and *Principal Component Analysis* (PCA) (further information can be found in [6, 7]).

2. Methods

We used, firstly, 19 industrial clinkers named from C1_1 to C6_19 (coming from different cement plants) and 7 laboratory clinkers (L1 to L7), given in Table 1. Optical microscopy nalysis has been made on all of these clinkers. Image segmentation has been made on resulting images within *ImageJ* environment by using various techniques, such as *Selection by color*, *Dilate*, *Erode*, *Threshold*, *Edge Detection* etc. synthesized in Figure 1. The image analysis block, conceptualized in dotted line, that is used to isolate the contours of the particles, will not be detailed here as it was already the subject of other papers [8, 9]. It is important to mention that the procedure had to be finely tuned for almost every clinker, mostly on *Threshold* value.

The main of the paper targets a very solid principle, widely accepted, namely: there is a correlation between composition and properties via structure (microstructure, in this case) [10]. This correlation can be sketched as in Fig. 1, as related to the aim of the paper. However, for the same composition, changes in how the material has been synthesized can lead to different microstructures and therefore the properties will change[11]. Because this causal relationship exist without being questioned, the immediate consequence is that that by a proper analysis of a *pivotal element* one can identify - in a given context – for example, previous activities and materials used (in this case we refer to *Composition* and/or *Processing* conditions) but it becomes also possible to predict material performance. In this paper, in the context of the scheme given in Figure 1, the *pivotal element* is represented by the analysis of the *Microstructure* of the material. Briefly said, once a comprehensive, relevant database has been constructed, one can *identify* clinkers or perform *diagnosis* or *process optimization*. This could be also an alternative or an addition to the *identification* of clinkers by trace elements – see [12] for an example of "*clinker fingerprinting*" by fuzzy methods.

It is important to state that, in our case, once the boundaries of the particles were defined, for several clinkers there was the need to reconstruct small parts of them, for example where hydration products have been formed; that has been done manually (interventions were limited to the size of a few pixels). Resulting images were then used to compute all three categories of parameters: *Shape Factors, Fractal Dimension and Uniformity Degree*.

3. Results and discussions

3.1. Particle shape parameters

Among shape parameters, we focused on *Circularity*, *Solidity* and *Feret diameter* (see Table 1). The reasons are i) other shape parameters showed no interesting correlation neither among them nor with the rest of the parameters to be further used and ii) they were found to be not influential on the database. A good correlation (R^2 = 0.91) has been obtained only between *Circularity* and *Solidity*.

Shape parameters are, at a certain extent, widely used. In our case, we deal with fairly rounded particles of belite but also with angular particles of alite, thus being complicated to compare images containing only belite with ones containing only alite. Framing a number of particles in clinker can imply that all particles placed on image edges cannot be used, though the space occupied by their fragments is useless, and information is lost – and they become important when particles are big. Also, the interstitial phase can be, sometimes, very difficult to be treated – if not impossible – by using shape parameters. As a consequence, there is the need for another parameter that can properly solve these issues. We used here the *Fractal Dimension*.

Table 1

Set A of parameters synthesizing both, images and grain size/shape parameters
Setul A cu imagini, factori de formă și parametri corelați cu granulometria particulelor

Clinker ID	Microscopy image	Grain boundaries	Circularity	Solidity	Feret diameter, µm	FD	U_H
C1_1	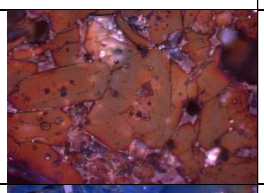	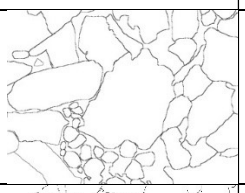	0.086	0.169	31	1.346	0.570
C1_2	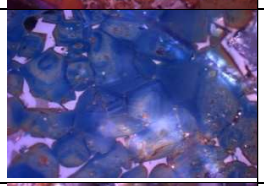	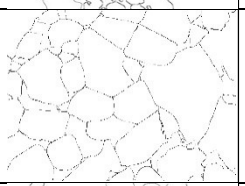	0.229	0.390	23	1.237	0.701
C1_3		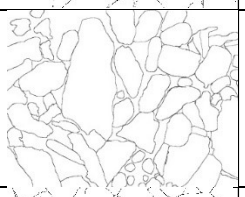	0.667	0.634	9	1.286	0.579
C1_4	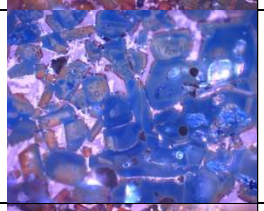	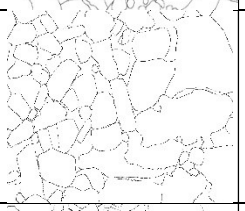	0.380	0.359	52	1.250	0.666
C1_5	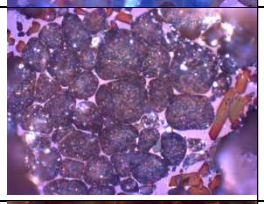	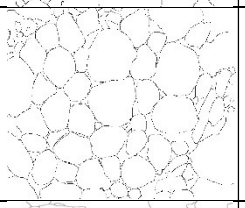	0.241	0.397	8	1.278	0.930
C3_6	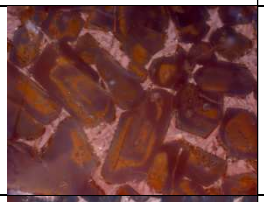	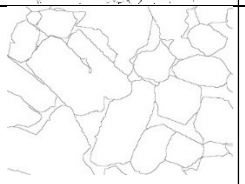	0.525	0.570	21	1.234	0.825
C3_7	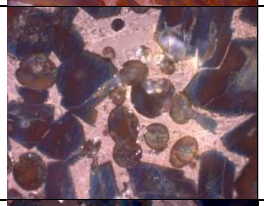	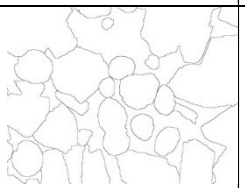	0.022	0.100	26	1.226	0.838
C3_8	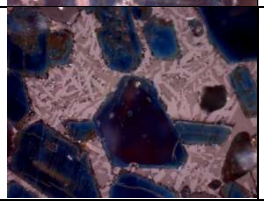	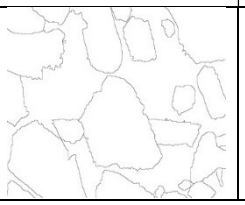	0.018	0.058	29	1.212	0.799

C3_9	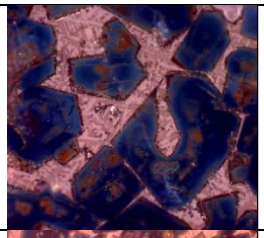	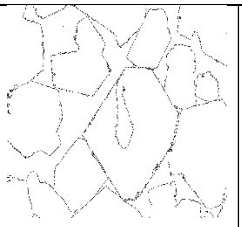	0.645	0.673	12	1.251	0.814
C3_10	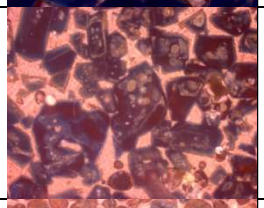	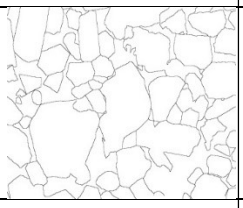	0.093	0.253	26	1.218	0.758
C3_11	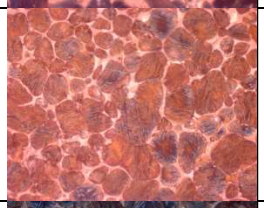	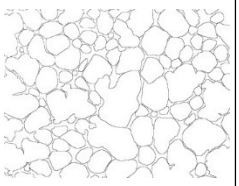	0.546	0.697	2	1.298	0.737
C3_12	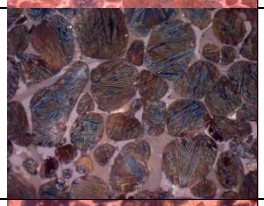	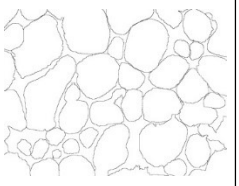	0.212	0.356	10	1.257	0.741
C3_13	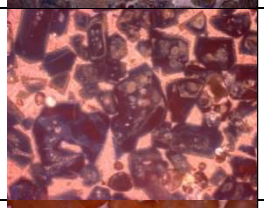	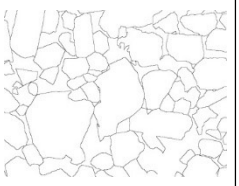	0.155	0.297	13	1.244	0.658
C4_14		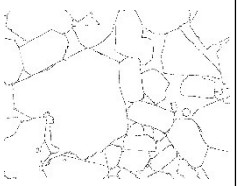	0.393	0.402	20	1.275	0.662
C4_15	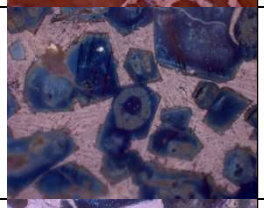	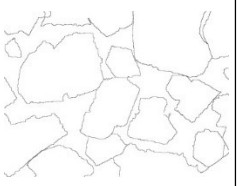	0.020	0.083	35	1.218	0.748
C4_16	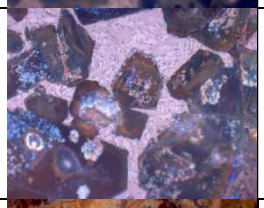	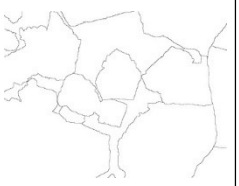	0.041	0.102	32	1.208	0.728
C4_17	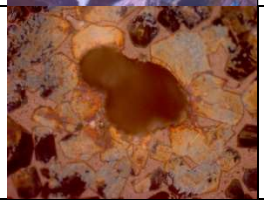	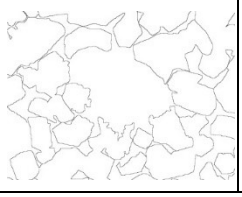	0.035	0.116	23	1.234	0.887

C6_18	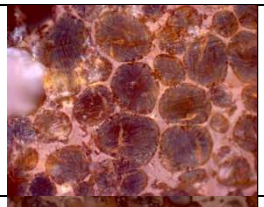	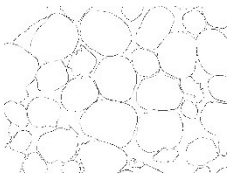	0.182	0.317	11	1.237	1.028
C6_19	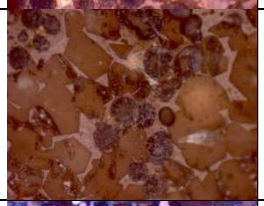	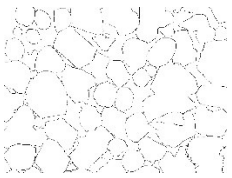	0.218	0.379	9	1.245	0.999
L1	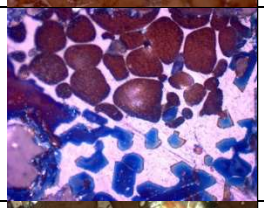	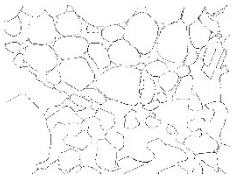	0.202	0.357	13	1.249	0.878
L2		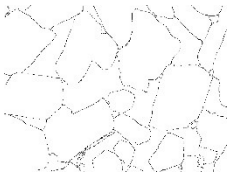	0.143	0.300	14	1.230	0.761
L3		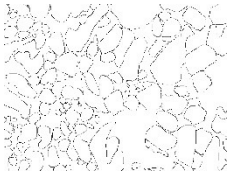	0.135	0.242	12	1.264	0.883
L4		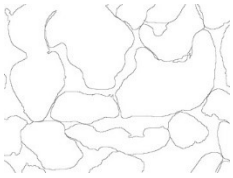	0.039	0.103	35	1.233	0.726
L5		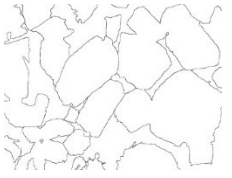	0.042	0.125	24	1.259	0.708
L6	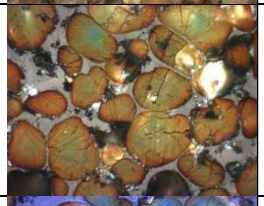	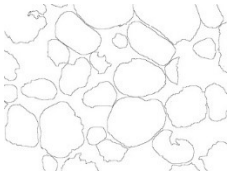	0.107	0.162	21	1.233	0.909
L7	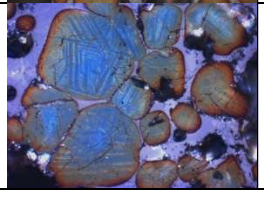	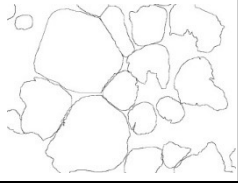	0.103	0.153	30	1.284	0.835

3.2. Fractal Dimension

Fractal Dimension (FD) can handle self-similar patterns and/or fractured (irregular) shapes. In our previous work [13], we successfully used *Fractal Dimension* to characterize highly irregular industrial trends; we are making here an extension of these concepts on populations of grains for

mineral phases in cement clinker that do possess neither self-similarity nor fractured contours.

There are multiple reasons why FD calculation could offer benefits, such as:

- the procedure is simple and reliable, provided statistically enough particles are used;
-
- we can use all features of the SEM or optical microscopy image, i.e. also the parts of the grains that are laid at the edge of the picture;
- it is correlated with both particles size and shapes (FD is inversely proportional with the average particles size, see Table 1);

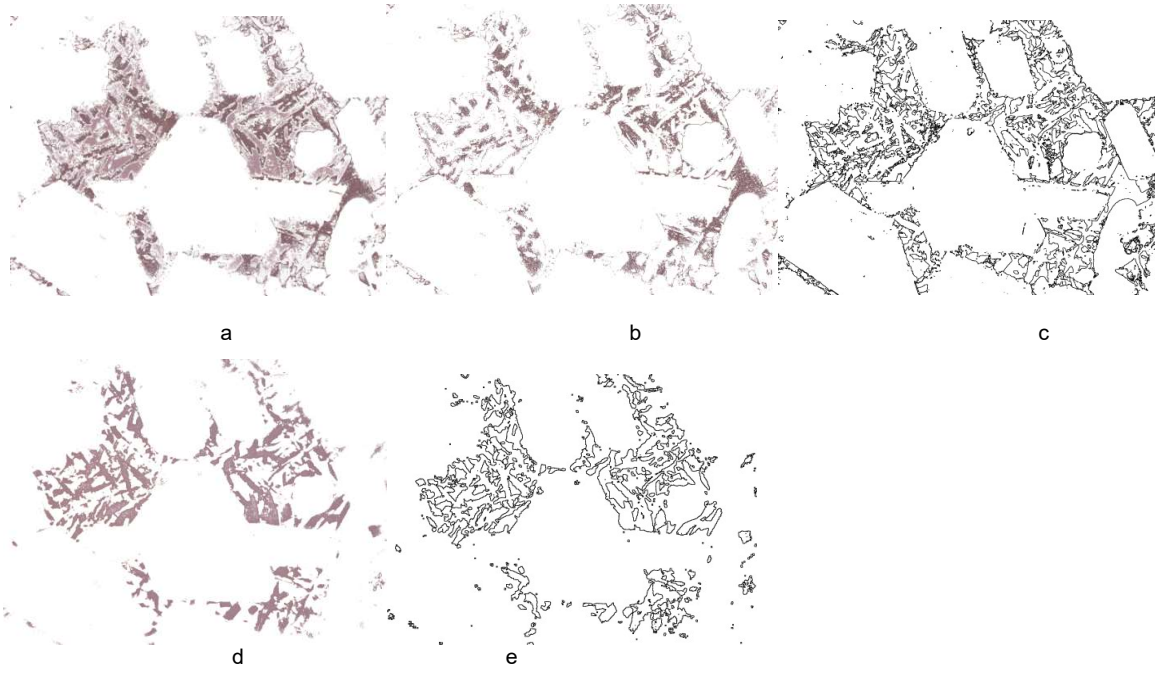

Fig. 2 - C3_8 clinker with selections of constituting minerals and grain boundaries. Remarks: a) IP containing C_3A and C_4AF, b) isolated C_3A, c) grain boundaries of C_3A (FD = 1.468), d) isolated C_4AF, e) grain boundaries of C_4AF (FD = 1.504) / *Clincherul C3_8 cu selecții ale mineralelor constituente și frontierele (izolate ale) particulelor. Observații: a) faza interstițială, FI, care conține C_3A și C_4AF, b) faza C_3A izolată, c) frontierele particulelor de C_3A (FD = 1.468), d) faza C_4AF izolată, e) frontierele particulelor de C_4AF (FD = 1.504).*

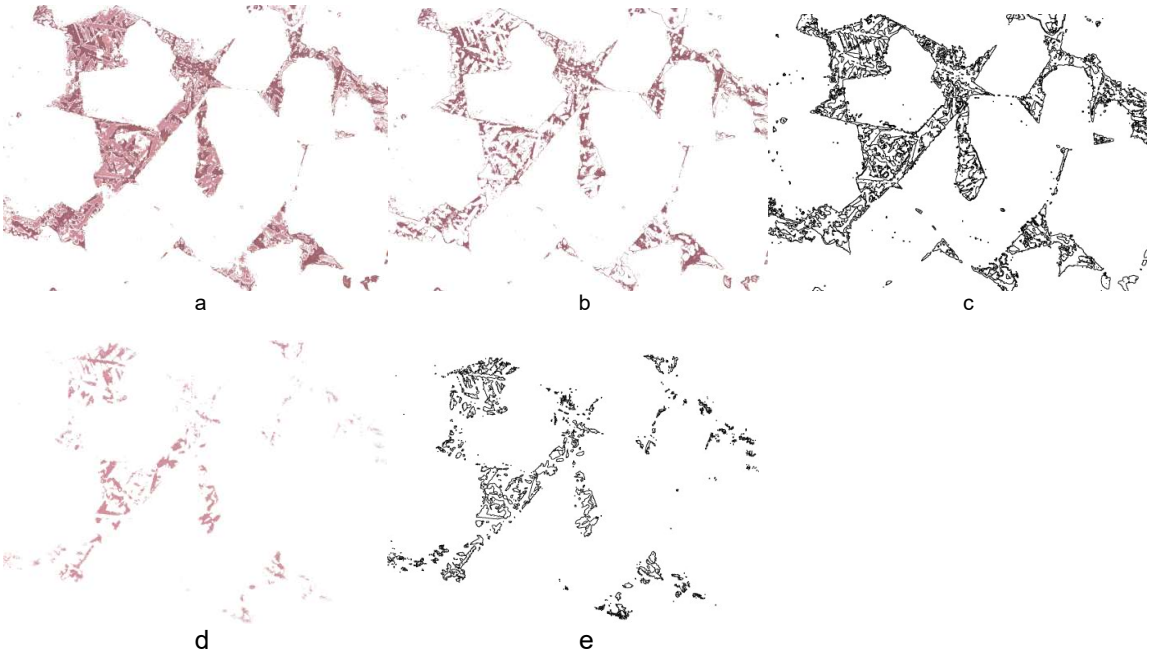

Fig. 3- C3_9 clinker with selections of constituting minerals and grain boundaries. Remarks: a) Alite and IP, b) isolated Alite (FD = 1.251), c) IP consisting of C_3A and C_4AF, d) isolated C_3A, e) grain boundaries of C_3A (FD = 1.353), f) isolated C_4AF, g) grain boundaries of C_4AF (FD = 1.4908) / *Clincherul C3_9 cu selecții ale mineralelor constituente și a frontierelor particulelor. Observații: a) alit și faza interstitială, b) Alit izolat (FD = 1.251), c) FI conținând C_3A și C_4AF, d) C_3A izolat, e) frontierele particulelor de C_3A (FD = 1.353), f) C_4AF izolat, g) frontierele particulelor de C_4AF (FD = 1.4908).*

- it is represented by a single value that can be further used (for example in correlations);
- in some particular cases such as a single-phase material it is quasi-invariant to the selected working area of the image, provided statistically enough particles are used in calculations;
- no confusion can be made, such as between particles and pores;
- in our situation, it can effectively describe also the *Interstitial Phase* (IP) and could be used to make distinction between different components of the IP.

To exemplify this last argument, we also applied the FD calculation to the interstitial phase of two clinkers, C3_8 and C3_9 (see Table 1). Interstitial phase consists in C_3A (tricalcium aluminate) and C_4AF (tetra-calcium aluminoferrite) intermixed minerals, therefore difficult to be examined (depending on cooling conditions, vitreous phase can also be found in IP). The IP and, then, C_3A and C_4AF constituents were carefully selected (by color) and the resulting images were processed according to the procedure sketched in Figure 1. FDs are then computed and compared. Results are given in Figures 2 and 3.

As compared of FD for the alite phase, which is 1.23, C_3A and C_4AF minerals exhibit higher values: C_4AF recorded about 1.50 for both clinkers while C_3A showed somehow different values, averaging about 1.41.

3.3. Uniformity degree

Particles size distributions can be associated with and well-described by some distribution functions (Laplace, exponential, Rosin-Rammler-Sperling etc.). There are, however, a series of practical issues related, basically, to the specificity of the distribution that prevents one to compare, in some cases, different distributions [14]. Also, along with specificity and, mostly, due to it, all fitting coefficients are empirically obtained, thus being complicated or even impossible to compare the uniformity degree of different distributions. All these difficulties can be overcome if one uses a parameter coming from informational statistics, i.e. *Shannon entropy*, *H*. *Shannon Entropy* evaluates the amount of order/disorder of a system.

Equation (1) gives the *Uniformity Degree*, U_H, for discrete particles distribution. U_H has been used in [14] to characterize cement powder particles and it was considered to be equivalent to *Shannon Entropy*, *H*. The difference is, in [14] the size distribution was continuous, and therefore an integral form of the Eq. (1) has been used.

$$U_H = -\sum_{i=1}^{n} f_i \cdot log_{\ i} \qquad (1)$$

where: $0 \le f_i \le 1, i = 1,\acute{n}, \sum_{i=1}^{n} f_i = 1$, n – number of size bins, f_i – relative frequencies.

U_H will be employed here to describe particle size distribution of the considered clinkers. The main idea is the higher the disorder – meaning the higher the differences between frequencies are, and the larger the distribution is (expressed as the number of size bins) – the higher the U_H is (see Fig. 4). Distribution shape – normal/multimodal etc. and/or discontinuous size distribution can also affect the value of the U_H.

Many techniques make the assumption that every particle is a sphere and report the value of some equivalent diameter. The averaged equivalent diameter can be further used to discover correlations within the causal *Composition...Properties* chain.

For every clinker in Table 1 there were measured all the particle areas with the aid of image analysis techniques [1,8,9], from which the averaged equivalent diameter resulted. Histograms of size distribution were made and frequencies f_i were computed from the size bins. U_H values were further obtained by using frequencies f_i with the aid of Eq. (1).

By cross-examining images, *FD* and U_H values and histograms interesting information has been drawn. For example, in Figure 4 are given histograms corresponding to extreme values of U_H. Clinker C1_1, having the smallest Shannon entropy, is made of very large alite grains and also a small number of belite grains that has the same size as the rest of the alite grains. On the opposite, clinker C6_18 has the highest Shannon entropy, which is explained by the existence of a far-from-normal particle size distribution (note the obvious difference between

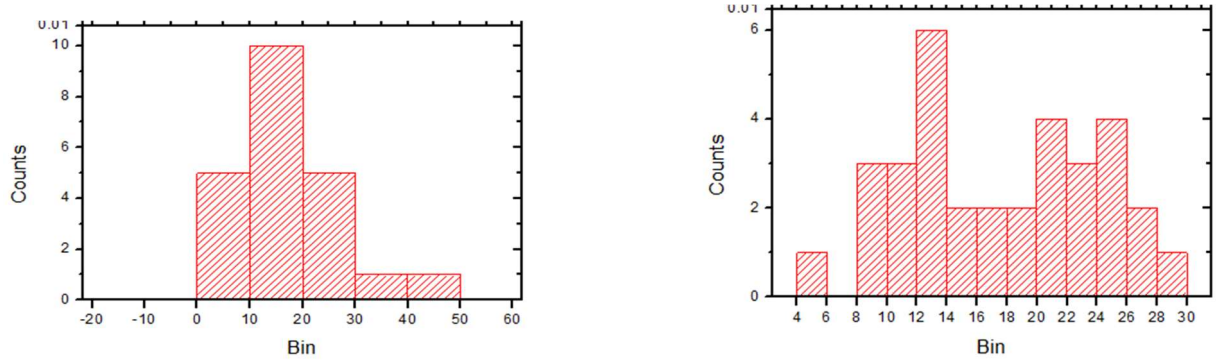

a) U_H = 0.570 b) U_H = 1.028

Fig. 4 - Particle size distribution for clinkers a) C1_1 and b) C6_18.
Distribuția granulometrică a clincherelor a) C1_1 și b) C6_18.

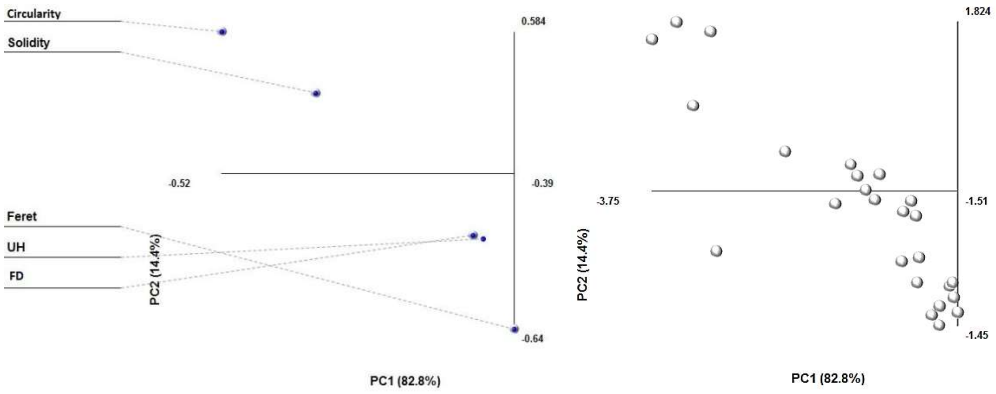

a) b)

Fig. 5 - Principal component analysis on Set A (a) Loadings; b) Score plot) explains the influence of the parameters *on* the datasets.
Analiza Componentelor Principale pentru Setul A a) Încărcări; b) Scoruri, evidențiază influența parametrilor asupra datelor.

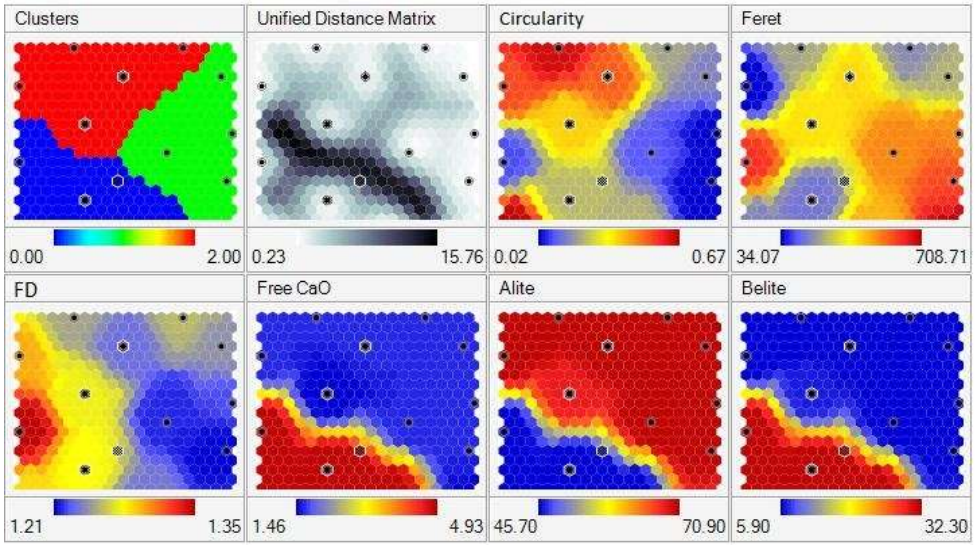

Fig. 6 - Self-Organizing Maps on *Set B* show similarities or opposite behaviors *between* parameters
SOM realizate pe Setul B evidențiază similarități sau comportamente opuse între parametri.

the two distributions). It is made of only belite grains. Therefore, we can infer that a small U_H is an indicator of a good transformation of belite in alite and of the growth of very large alite crystals, while high values of U_H can be correlated with the existence of mainly or only, belite crystals. However, for itself, this parameter cannot explain everything: clinker C6_19 contains almost equal proportions of alite and belite crystals yet it has a U_H value of 0.999 (a high value). So, as no parameter can explain by itself all results, it becomes necessary to correlate them.

3.4. Multivariate Analysis (MVA) results

3.4.1. MVA on industrial clinkers

PCA has been performed on *Set A* of parameters and the results were given in Figure 5. Among shape and/or size parameters used here, U_H and *FD* exhibit a similar influence, being very close to each other. However, by corroborating the *Loadings* with *Score* plots, it could be inferred that some data can be explained by one or by a combination of size/shape parameters. This statement is based on the similarity between the general patterns of the two plots. Circularity plays the most important role on both Principal Components (PCs), although only 3-4 records can be explained by this shape parameter alone. The rest of the records are scattered in the area controlled by U_H and *FD*, while another cluster is explained mainly by the influence of Feret diameter.

Nevertheless, the 25 clinkers are very different: some of them are industrial clinkers (16) while the rest are laboratory made (7). Also, the industrial clinkers were obtained in different conditions, i.e. by using different fuels; specifically, conventional with different amounts of – different – alternative fuels (alternative fuels were substituting 10-15% of conventional fuels). Accordingly, they were grouped into 5 categories. It was at least supposed - if not expected - that these categories could be clearly identified in the Score plot, yet clinkers were scattered here without any tendency to respect other pattern than the one given by the position of the parameters. A first conclusion is: microstructural features of the clinker crystals

cannot be exhaustively described by only one parameter but by a range of parameters. The second one is: there is the need for more information to be able to classify records by their origin. Thus, we further introduced in the analysis the clinker composition. Clinkers C1_1-C1_5 were selected for having the highest *free CaO* (up to 4.93%), the lowest alite (≥45.7%) and belite up to 32.3%. Clinkers C3_6-C3_13 had the *free CaO* closely averaging 1.63%, alite up to 70.9% and belite at least 5.9%. Clinkers C4_14-C4_17 had the lowest *free CaO* of 1.46%, alite 68.7±2.4% and belite of at least 5.9%. Ranges corresponding to each mineral in clinker are given in Fig. 6. Clinkers C6_18, C6_19 and L1-L7 had no chemical and mineralogical analysis results; therefore they were not used furthermore.

In order to introduce new information, we made another configuration of parameters, called *Set B*. In this *Set B*, parameter U_H was excluded because it has a very similar, already known behavior to *FD*, thus providing no new information. Also, *Solidity* has been removed after several trials with it been used or been excluded: no notable influence on all of the analysis results in the newest parameters configuration has been observed (note that *Solidity* was found to be strongly correlated with *Circularity*, see Fig. 1). It is important to keep the number of parameters used in the analysis as low as possible, as they are notoriously not easily available on a regular basis. Here we used a heuristic approach to identify the optimal/best set of parameters.

We trained a *Self-Organizing Map* (SOM) with parameters from Table 1, for clinchers C1_1 to C4_17. The classification of the training data was made with the aim of finding similarities (or dissimilarities) between parameters that were used. We learned that, without a doubt, belite and *free CaO* have similar behaviors while being both opposite to alite. It is very easy to explain this based on the visual analysis of the Fig. 6. A confirmation of this last observation came from the PCA analysis shown in Fig. 7: alite and the well-grouped *free CaO* – belite are opposite on PC1 and they are all important. *Circularity* is very little affected on PC1 but becomes more important on PC2, compared to previous PCA results – Figure 5; *Fractal Dimension* show an average influence on data on both PCs, being placed very close to the intersection of the PCs.

Score plot reveals, in that case, that data are very well placed in clearly-defined and distinct clusters, corresponding to the clinker classes they belong (C1, C3 and C4- see Table 1). Clusters are placed on the PC1 according to their free CaO-belite/alite content i.e. they are explained by these parameters. For example, a very high content in belite and free CaO will place the clinker in class C1, while, if the alite content is high, it could be a candidate for C3 or C4 classes. That observation is very important on a larger scale: one can easily place/identify/recognize a clinker by the parameters used here, without knowing anything about how the clinker has been processed (about the raw materials, fuels used, process control strategy), provided enough data are available. In other words, by constructing a proper database we can place (*identify*) an unknown clinker in one cluster by using this very simple technique. Within each cluster, data is explained due to *Feret diameter* and *Circularity*. For example, if *Feret diameter* is high, the clinker will fall below the PC1 axis, otherwise it will be placed above.

3.4.2. MVA on laboratory made clinkers

A question should be put at this point: what if clusters themselves cannot be always clearly defined *and* distinct? To exemplify that, we made seven clinkers in laboratory by using different processing conditions – see Table 2. Three classes of clinker were obtained from different raw meals (denoted A, B and C); the oxide composition of the raw meals ranged within 42.80–43.32% CaO, 12.57–13.87% SiO_2, 3.85–4.24% Al_2O_3, 2.06–2.69% Fe_2O_3, via different thermal histories (various processing time and temperature). Free CaO was determined on the resulted clinkers; we than made the image analysis of the microstructure and performed the calculation of the *FD* (also given in Table 2).

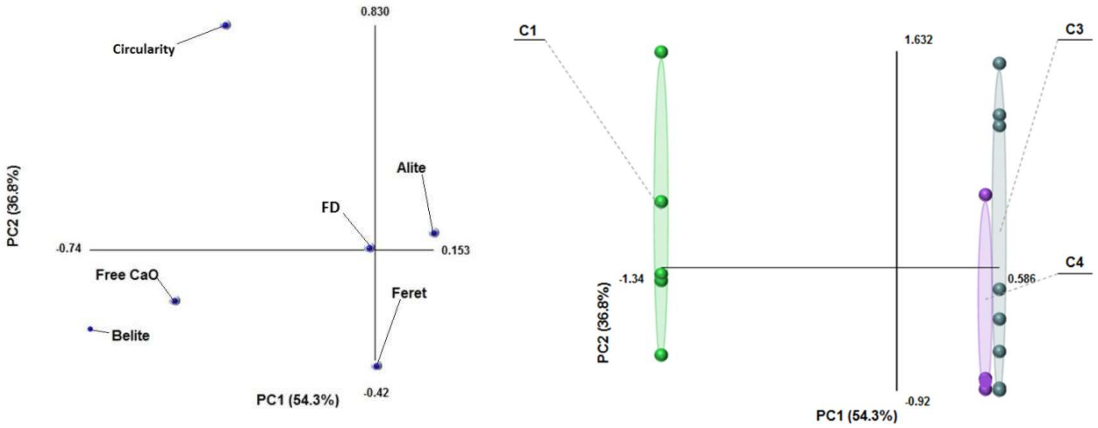

a) Loadings b) Scores

Fig. 7- PCA on data in *Set B*. Distinct clusters of data were found, being well explained by size/shape parameters.
PCA aplicat pentru Setul B de date. Sunt identificate clustere de date bine corelate cu factorii de formă/granulometria.

Table 2

Set C of data
Setul C de date

Clinker ID	t, min	T, °C	FD	fCaO, %	Clinker class
P1	60	1450	1.274	0.56	B
P2	20	1450	1.324	0.47	C
P3	60	1450	1.328	0.22	C
P4	30	1350	1.340	6.96	A
P5	30	1350	1.274	3.71	B
P6	20	1450	1.316	1.99	B
P7	20	1450	1.356	0.78	C

PCA analysis shown in Figure 8 reveals that only two factors are really significant for identifying the pattern of correlations: *free CaO (fCaO)*, which is the most important of them, and the processing time, *t*. *T* denotes processing temperature. Also, classes A and C are both well-defined and distinct and their positioning along PC1 is properly explained by the value of the *free CaO*. For class B, clinkers are scattered along PC1 due to the influence of the processing conditions. Specifically, the clinker situated on the positive area of the PC1 is clinker P5, which has a high content of *free CaO* (the highest among its class) due to poor processing conditions (see Table 2). The clinker that lay at the negative area of both PCs, being also very close to another clinker that belongs to class C (clinker P3), is clinker P1. Both clinkers P1 and P3 were thermally treated at the highest temperature (1450°C) and for the highest processing time (60 min), thus resulting in two similar clinkers from the viewpoint of *free CaO* content. However, microstructure analysis, given by the value of the FD, differentiates these two clinkers even if the influence of the *FD* within the global picture, for this case, is an average one. It has to be mentioned that *T* and *FD* have a mutual, entangled influence over the other parameters – if they are removed from the database, results become very poor.

Coming back from the question regarding adjacent (or even, sometimes, superimposed) clusters, one should observe that in both cases, for clinkers belonging to *Set B* and *Set C*, the *free CaO* is a main parameter of influence over data variability on the most important PC, i.e. PC1. In both Sets the analysis was statistically relevant for the variability of the data (54.3% on PC1 and 36.8% on PC2 for *Set B* - more than 91% cumulated - and 84.6% on PC1 and 15.3% on PC2 for *Set B* – almost 100%).

Another observation to be retained is that, if a clinker is known – for example we know the clinker class, the raw materials and fuels used, but not the process control strategy – and it doesn't fit in the cluster corresponding to its class, we can suspect an alteration of one or more process parameters (this alteration was spotted by PCA analysis in the case of *Set B* of the laboratory made clinkers belonging to class C). Thus is becoming important, at this moment, to further introduce and to corroborate with the analysis of the process parameters (denoted *Set D*).

3.4.3. MVA on industrial process parameters

Clinkering plant process control deals with tens of parameters about material, air, fuel, flue gas and about the installation itself, seen as temperatures, pressures, power etc. that are monitored or controlled. These parameters are sometimes intertwined, therefore their influence on the process and, consequently, on the clinker quality is a complicated one. Our previous experience with clinkering plant process analysis [6] revealed that, to be successful in identifying correlations within a process parameters database, that one should contain at least 500 valid and relevant records, while parameters have to be chosen by an intricate analysis.

In our analysis we refer a database made of 738 records that were collected from a clinkering plant based on the dry process technology the same period of time the clinkers were collected.

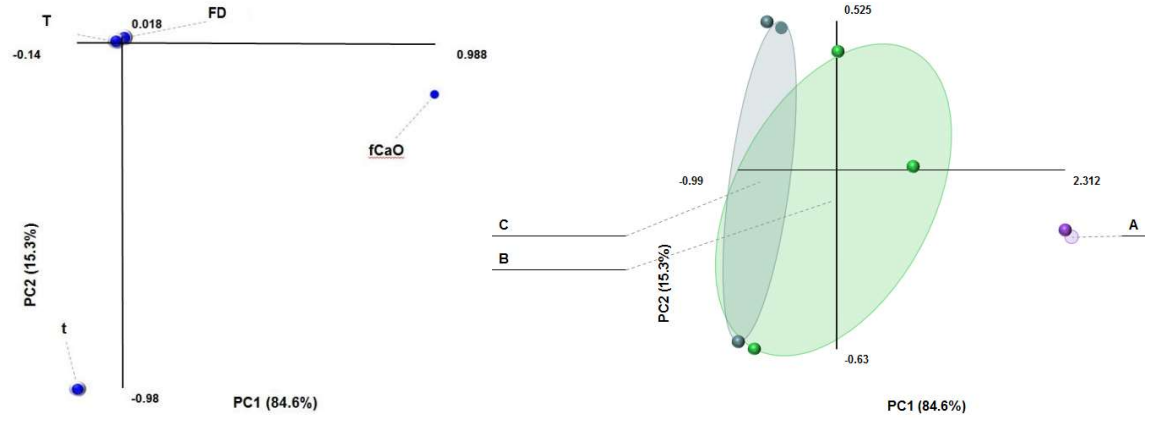

Fig. 8 - PCA performed on *Set C* reveal superimposed clusters but, also, the importance of the *free CaO* content (denoted *fCaO*) / *PCA realizată pe Setul C evidențiază clustere suprapuse parțial dar și importanța CaO liber (denumit fCaO).*

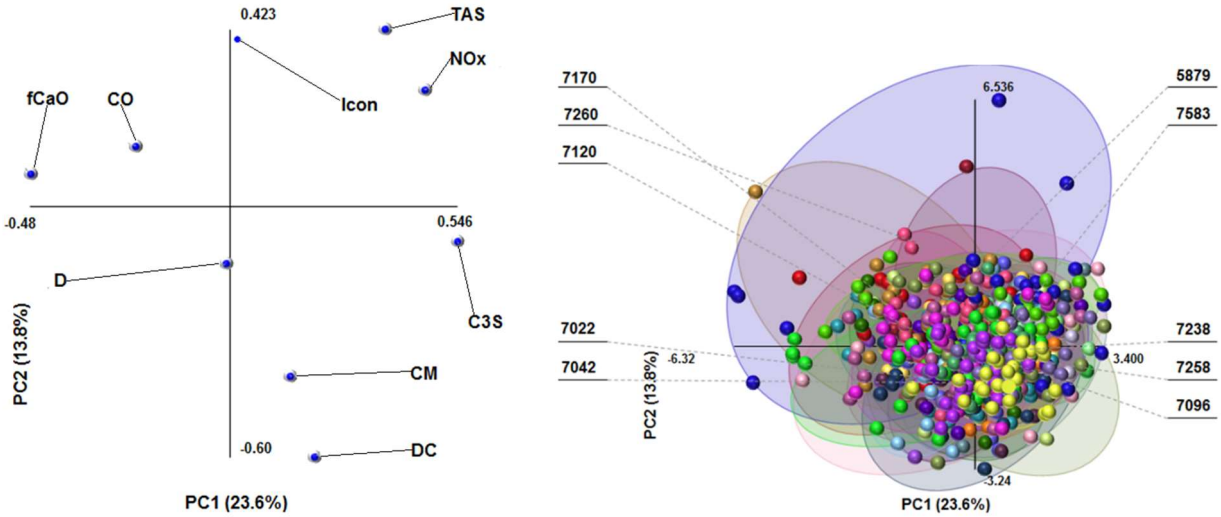

Fig. 9 - PCA performed on selected process parameters. Data has been categorized by LCV / *PCA realizată pentru parametrii de process selectați. Datele au fost împărțite automat pe categorii pe baza valorii puterii calorifice inferioare.*

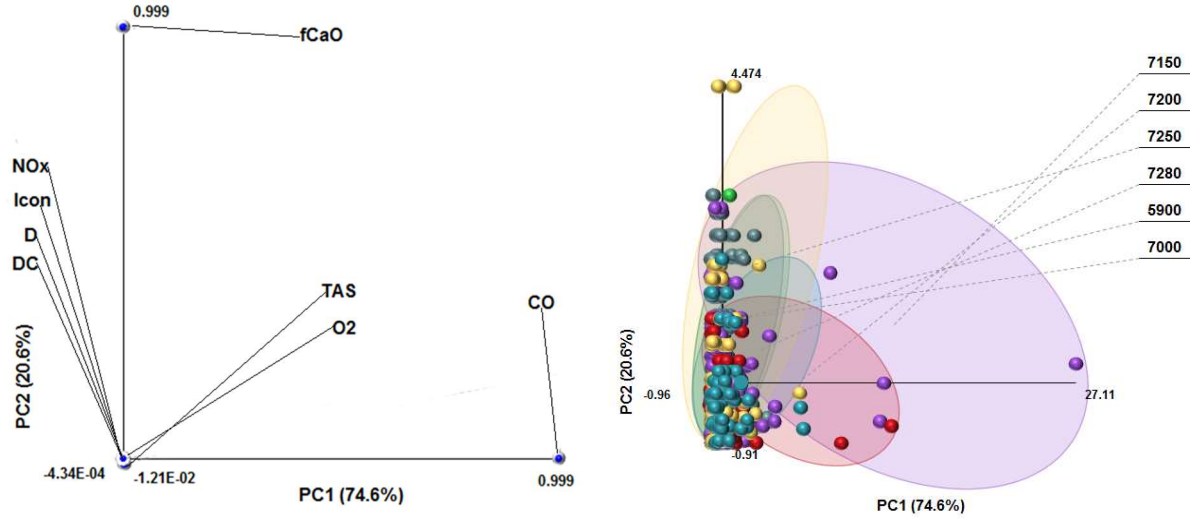

Fig. 10 - PCA performed on a reviewed selection of process parameters. *Free CaO* and *CO* contents were found to be influential on process data / *PCA realizată pentru o selecție a parametrilor de proces. CaO liber și conținutul în CO în gazele de ardere exercită cea mai importantă influență asupra datelor.*

The records refer to process parameters, oxide and mineral compositions. Also, the *Low Calorific Value* (LCV) of the fuel was known.

Based on our previous experience [6], we selected the process parameters through a heuristic approach. The process parameters here show no evolutions but only ordinary fluctuations, which is desirable from the point of view of the process control.

- In a first stage, gas analysis (*CO*, NO_x in ppm), fuel intake (*DC*, kg/h), clinker analysis (*free CaO*, C_3S, in %), kiln torque (*CM*, %), clinker cooler crusher power (*Icon*), pressure made by the exhaust gases fan (*D*, N/m^2) and temperature of the secondary air (*TAS*, in °C) were used. Except for the clinker analysis data (*free CaO*, C_3S), all other parameters were used in paper [6]. We performed PCA on data categorized by their LCV value. Here the LCV is given in kcal/kg of solid fuel, which is a combination of petcoke and alternative fuels in much lower amounts (<15%); LCV values only play the role of category labels. Results of the PCA can be found in Figure 9.

Loadings plot could be comfortably interpreted from a technological point of view. *TAS* and NO_x are normally related, such as if one increases so do the other. When the air temperature (*TAS*) is high, then C_3S and NO_x are also high while *fCaO* is low. And inversely. It is known that, if NO_x is high, then *CO* is low (and inversely). These findings are consistent to our previous research [6]; however, data variability is explained only to an extent of less than 40% (specifically 23.6 + 13.8%). The *Score* plot does not help us to understand and find correlations as no pattern can be extracted from

it, i.e. no apparent order can be found in score plots - see (Fig. 9). Therefore, a thorough investigation was required.

- In a second attempt we removed C_3S and CM and we introduced O_2 content in flue gas; we performed PCA and the results plotted in Figure 10. There were no technological considerations that conducted to these situations; all changes in selecting parameters were made in a heuristic approach.

Correlating the loadings and the score plots means to identify – if any – favored directions in which one could found an evolution. Two directions are predominant in both plots in Figure 10 and these preferred directions correspond to the two most influential parameters: on the abscissae, that explains 74.6% of the data variability, *CO* is the single parameter that have a really high value (0.999) while the rest of the variables that are shown on that axis do not influence otherwise but moderate (their values are around the origin). Only a little number of samples vary notably along with that axis; however, their role is very important because they have a very high value on PC1 which explains about ¾ of the data. It is important to state that the rest of the parameters show a mutual, undetected influence over the database – without any of them the efficiency will drop (as it was observed in the first attempt). On the ordinate axis, accounting for 20.6% of the variability of data, it could be much easier to understand what makes the samples different, i.e. what variable influences them. In the *Loadings* plot one can observe – the same as in the abscissae case – that there is only one variable that has a significant value of 0.999, the *fCaO* variable. The samples of all categories are very well grouped along this axis; this remark allow one to conclude that *fCaO* can be an efficient tool used to *differentiate* and even *identify* clinkers (provided enough data are available).

4. Conclusions

A rigorous and reasonably simple procedure has been described and successfully applied to find correlation between composition, processing conditions and microstructure for different clinkers, both industrials and laboratory made. Various parameters such as chemical analysis of the raw materials, clinkers, process parameters, information from *image analysis* on clinker micrographs were used in *Principal Component Analysis* and *Self-organizing maps* to extract information. It was found that the link between these different categories of data is the *free CaO* content in clinker. *Fractal dimension* and a Shannon Entropy based parameter, called *Uniformity degree*, have successfully described microstructure of the clinkers. *Fractal dimension* includes information about both size and particle morphology while the *Uniformity degree* characterizes the particle size distribution; however, these two parameters were found, through analysis, to have a similar behavior.

It is expected that the procedure used here can help to position an unknown clinker, given a minimal set of laboratory results, on, for example, *Principal Component Analysis* plots, if a *relevant* database was used in the analysis. The procedure given in the paper can be used on any material, on optical microscopy or SEM images, with very little adjustments.

Efforts should be further made to incorporate also the *Properties*, more specifically, the *Compressive Strength* of the cement. It is expected that results will gain in clarity, provided a relevant database will be available.

Acknowledgements

This work was done through the support of Partnerships in priority areas program - PNII, developed with the support of MEN - UEFISCDI, Romania, project no. 223 „Advanced optimization process of cement manufacturing in condition of waste recovery (AWARE)".

PCA was performed using the Excel add-in Multibase package (Numerical Dynamics, Japan). SOM analysis was performed using Peltarion Synapse. Image analysis has been made by using ImageJ tools.

REFERENCES

1. S.T. Erdoğan, X. Nie, P.E. Stutzman, E.J. Garboczi. Micrometer-scale 3-D shape characterization of eight cements: Particle shape and cement chemistry, and the effect of particle shape on laser diffraction particle size measurement, Cem. Concr. Res., 2010, **40**, 731.
2. S. J. Blott, K. Pye. Particle shape: a review and new methods of characterization and classification, Sedimentology, 2008, **55**, 31.
3. I.Vecchio, K. Schladitz. 3D Geometric characterization of particles applied to technical cleanliness, Image Anal. Stereol, 2012, 31, 163.
4. G. Landini. Fractals in microscopy, J. Microscopy, 2011, 241, 1.
5. P. LI, Q. ZHANG, K XUE. Fractal Characteristics and Prediction of Ti-15-3 Alloy Recrystallized Microstructure, J. Mater. Sci. Technol., 2008, **24**(6), 836.
6. Z. D. Ghizdăveţ, Knowledge discovery in industrial datasets. Application. Part I – Analysis, Rom. J. Mater., 2010, **40** (2), 161.
7. Z. D, Ghizdăveţ, Knowledge discovery in industrial datasets. Application. Part II – Prediction, Rom. J. Mater., 2011, **41** (1), 73.
8. P. Stutzman. Scanning electron microscopy imaging of hydraulic cement microstructure, Cem. Concr. Compos., 2004, **26**, 957.
9. R. M Carter, Y Yan. Measurement of particle shape using digital imaging techniques, J. Physics: Conference Series, 2005, **15**, 177.
10. H. Khanbareh, X. Wu, S. van der Zwaag. Analysis of the fractal dimension of grain boundaries of AA7050 aluminum alloys and its relationship to fracture toughness, J. Mater. Sci, 2012, **47**, 6246.
11. M. Tanaka, M. Komagata, M. Tsukada, H. Kamiya. Fractal analysis of the influence of surface roughness of toner particles on their flow properties and adhesion behavior, Powder Technol., 2008, **186**, 1.
12. F.D. Tamás, J. Abonyi, Trace elements in clinkers – II. Qualitative Identification by Fuzzy Clustering, Cem. Concr. Res., 2002, **32**, 1325.
13. Z. D, Ghizdăveţ, R, Grădinaru, Heat balance computation on a clinkering plant over different time steps, Rom. J. Mater., 2012, **43** (3), 332.
14. D. Radu, Z. D, Ghizdăveţ, Relationships between specific surface area and particle size uniformity for disperse powdered materials, Rom. J. Mater., 2015, **45** (4), 384.